# Resonant tunneling into a quantum dot embedded inside a microcavity

Yueh-Nan Chen* and Der-San Chuu†
*Department of Electrophysics, National Chiao Tung University, Hsinchu 30050, Taiwan*
(Received 19 June 2002; published 29 October 2002)

We propose to measure the Purcell effect by observing the current through a semeiconductor quantum dot embedded in a microcavity. An electron and a hole are injected separately into the quantum structure to form an exciton and then recombine radiatively. The stationary current is shown to be altered if one varies the cavity length or the exciton energy gap. Therefore, the Purcell effect can be observed experimentally by measuring the current through the quantum structure. In addition, we also find that super-radiance of excitons between quantum dots may also be observed in an electrical way.

DOI: 10.1103/PhysRevB.66.165316 PACS number(s): 78.67.−n, 42.50.Fx, 73.23.Hk

Recently, much attention has been focused on the enhanced spontaneous emission (SE) rate of the quantum dot exciton in an optical microcavity. Historically, the idea of controlling the SE rate by using a cavity was introduced by Purcell.[1] Considering the interaction between the atomic dipole and the electromagnetic fields inside a cavity, the SE rate can be expressed as $(2\pi/\hbar)\ \rho_{\mathrm{cav}}(\omega)|\langle f|V|i\rangle|^2$ , where $\rho_{\mathrm{cav}}(\omega)$ and $V$ are the photon density of states and atom-vacuum field interaction Hamiltonian, respectively. For a planar cavity with distance $L_c$ between two mirrors, the photon density of states is $N_c\omega/2\pi c^2$, where $N_c$ is an integer less than $2L_c/\lambda$. Thus, by varying the cavity length $L_c$, the SE rate can be altered. The enhanced and inhibited SE rate for the atomic system was intensively investigated in the 1980's (Refs. 2–5) by using atoms passed through a cavity.

Turning to semiconductor systems, the electron-hole pair is naturally a candidate for examining the spontaneous emission. However, as is well known, the excitons in a three-dimensional (3D) system will couple with photons to form polaritons—the eigenstate of the combined system consisting of the crystal and the radiation field which does not decay radiatively.[6] Thus, in a bulk crystal, the exciton can only decay via impurity, phonon scatterings, or boundary effects. The exciton can render radiative decay in lower-dimensional systems such as quantum wells, quantum wires, or quantum dots as a result of broken symmetry. The decay rate of the exciton is superradiant enhanced by a factor of $\lambda/d$ in a 1D system[7] and $(\lambda/d)^2$ for the 2D exciton polariton,[8,9] where $\lambda$ is the wavelength of emitted photon and $d$ is the lattice constant of the 1D system or the thin film. The super-radiance of excitons in these quantum structures have been investigated intensively.[10–13]

With the advances of modern fabrication technology, it has become possible to fabricate the planar microcavities incorporating quantum wells[14] or quantum wires.[15] In these systems it is possible to observe the modified spontaneous emission rate of excitons. Similar to its decay-rate counterpart, the frequency shift of a quantum wire exciton should also be modified in a planar microcavity. By using the renormalization procedure proposed by Lee *et al.*,[16] we have recently shown that the frequency shift shows discontinuities at resonant modes.[17] Instead of one-dimensional confinement of photon fields, experimentalists are now able to fabricate the quantum dot systems in laterally structured microcavities that exhibit photon confinement in all three dimensions.[18,19] Both inhibition and enhancement of the spontaneous emission of quantum dot excitons have been observed.[20] In this paper, a relatively simple way to observe the enhanced spontaneous emission is proposed to embed the quantum ring or the quantum dot in a microcavity.[21] By injecting electron and hole into the quantum dot, a photon is generated by the recombination of the exciton. This process allows one to determine Purcell effect by measuring the current through the quantum dot.

In our model, we consider a quantum dot embedded in a $p$-$i$-$n$ junction, which is similar to the device proposed by O. Benson *et al.*[21] The energy-band diagram is shown in Fig. 1.

Both the hole and electron reservoirs are assumed to be in thermal equilibrium. For the physical phenomena we are interested in, the Fermi level of the $p(n)$-side hole (electron) is slightly lower (higher) than the hole (electron) subband in the dot. After a hole is injected into the hole subband in the quantum dot, the $n$-side electron can tunnel into the exciton level because of the Coulomb interaction between the electron and hole. Thus, we may assume three dot states

$$|0\rangle=|0,h\rangle,$$

$$|U\rangle=|e,h\rangle,$$

$$|D\rangle=|0,0\rangle, \tag{1}$$

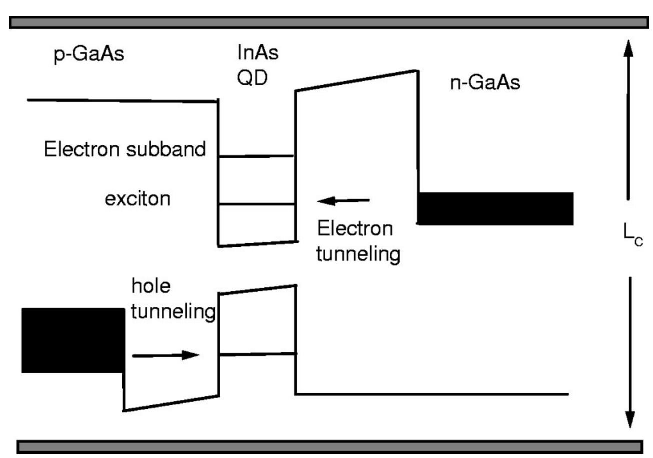


FIG. 1. Energy-band diagram of the structure.

 

where $|0,h\rangle$ means that there is one hole in the quantum dot, $|e,h\rangle$ is the exciton state, and $|0,0\rangle$ represents the ground state with no hole and electron in the quantum dot. One might argue that one cannot neglect the state $|e,0\rangle$ for a real device since the tunable variable is the applied voltage. This can be resolved by fabricating a thicker barrier on the electron side so that there is little chance for an electron to tunnel in advance. Moreover, the charged exciton and biexcitons states are also neglected in our calculations. This means a low injection limit is required in the experiment.[22] We can now define the dot operators $\hat{n}_U \equiv |U\rangle\langle U|$, $\hat{n}_D \equiv |D\rangle\langle D|$, $\hat{p} \equiv |U\rangle\langle D|$, $\hat{s}_U \equiv |0\rangle\langle U|$, $\hat{s}_D \equiv |0\rangle\langle D|$. The total Hamiltonian $H$ of the system consists of three parts: the dot Hamiltonian, the photon bath, and the electron (hole) reservoirs

$$H = H_0 + H_T + H_V,$$

$$H_0 = \varepsilon_U \hat{n}_U + \varepsilon_D \hat{n}_D + H_p + H_{\mathrm{res}},$$

$$H_T = \sum_k g(D_k b_k^\dagger \hat{p} + D_k^* b_k \hat{p}^\dagger) = g(\hat{p}X + \hat{p}^\dagger X^\dagger),$$

$$H_p = \sum_k \omega_k b_k^\dagger b_k,$$

$$H_V = \sum_{\mathbf{q}} (V_{\mathbf{q}} c_{\mathbf{q}}^\dagger \hat{s}_U + W_{\mathbf{q}} d_{\mathbf{q}}^\dagger \hat{s}_D + \text{c.c.}),$$

$$H_{\mathrm{res}} = \sum_{\mathbf{q}} \varepsilon_{\mathbf{q}}^U c_{\mathbf{q}}^\dagger c_{\mathbf{q}} + \sum_{\mathbf{q}} \varepsilon_{\mathbf{q}}^D d_{\mathbf{q}}^\dagger d_{\mathbf{q}}. \tag{2}$$

In the above equation, $b_k$ is the photon operator, $gD_k$ is the dipole coupling strength, $X = \Sigma_k D_k b_k^\dagger$, and $c_{\mathbf{q}}$ and $d_{\mathbf{q}}$ denote the electron operators in the left and right reservoirs, respectively. Here, $g$ is a constant with a unit of the tunneling rate. The couplings to the electron and hole reservoirs are given by the standard tunnel Hamiltonian $H_V$, where $V_{\mathbf{q}}$ and $W_{\mathbf{q}}$ couple the channels **q** of the electron and the hole reservoirs. If the couplings to the electron and the hole reservoirs are weak, then it is reasonable to assume that the standard Born-Markov approximation with respect to these couplings is valid. In this case, one can derive a master equation from the exact time evolution of the system. The equations of motion can be expressed as (see Ref. 22)

$$\langle \hat{n}_U \rangle_t - \langle \hat{n}_U \rangle_0 = -ig\int_0^t dt' \{\langle \hat{p} \rangle_{t'} - \langle \hat{p}^\dagger \rangle_{t'}\} + 2\Gamma_U \int_0^t dt' (1 - \langle \hat{n}_U \rangle_{t'} - \langle \hat{n}_D \rangle_{t'}),$$

$$\langle \hat{n}_D \rangle_t - \langle \hat{n}_D \rangle_0 = -ig\int_0^t dt' \{\langle \hat{p} \rangle_{t'} - \langle \hat{p}^\dagger \rangle_{t'}\} - 2\Gamma_D \int_0^t dt' \langle \hat{n}_D \rangle_{t'},$$

$$\langle \hat{p} \rangle_t - \langle \hat{p} \rangle_t^0 = -\Gamma_D \int_0^t dt' e^{i\varepsilon(t-t')} \langle X_t X_{t'}^\dagger \tilde{p}(t') \rangle_{t'} - ig\int_0^t dt' e^{i\varepsilon(t-t')} \{\langle \hat{n}_U X_t X_{t'}^\dagger \rangle_{t'} - \langle \hat{n}_D X_{t'}^\dagger X_t \rangle_{t'}\},$$

$$\langle \hat{p}^\dagger \rangle_t - \langle \hat{p} \rangle_t^0 = -\Gamma_D \int_0^t dt' e^{-i\varepsilon(t-t')} \langle \tilde{p}^\dagger(t') X_{t'} X_t^\dagger \rangle_{t'} + ig\int_0^t dt' e^{-i\varepsilon(t-t')} \{\langle \hat{n}_U X_{t'} X_t^\dagger \rangle_{t'} - \langle \hat{n}_D X_t^\dagger X_{t'} \rangle_{t'}\}, \tag{3}$$

where $\Gamma_U = 2\pi \Sigma_{\mathbf{q}} V_{\mathbf{q}}^2 \delta(\varepsilon_U - \varepsilon_{\mathbf{q}}^U)$, $\Gamma_D = 2\pi \Sigma \mathbf{q} W_{\mathbf{q}}^2 \delta(\varepsilon_D - \varepsilon_{\mathbf{q}}^D)$, and $\varepsilon = \varepsilon_U - \varepsilon_D$ is the energy gap of the quantum dot exciton. Here, $\tilde{p}(t') = p e^{i\varepsilon t} X_{t'}$, and $X_{t'}$ denotes the time evolution of $X$ with $H_p$. The expectation value $\langle \hat{p}^{(\dagger)} \rangle_t^0$ describes the decay of an initial polarization of the system and plays no role for the stationary current. Therefore, we shall assume the initial expectation value of $\hat{p}^{(\dagger)}$ vanishes at time $t=0$.

As can be seen from Eq. (3), there are terms such as $\langle \hat{n}_U X_t X_{t'}^\dagger \rangle_{t'}$ which contain products of dot operators and photon operators. If we are interested in small coupling parameters here, a decoupling of the reduced density matrix $\tilde{\rho}(t')$ can be written as

$$\tilde{\rho}(t') \approx \rho_{ph}^0 \mathrm{Tr}_{ph} \tilde{\rho}(t'). \tag{4}$$

By using the above equation, we obtain

$$\mathrm{Tr}[\tilde{\rho}(t') \hat{n}_U X_t X_{t'}^\dagger] \approx \langle \hat{n}_U \rangle_{t'} \langle X_t X_{t'}^\dagger \rangle_0 \tag{5}$$

and correspondingly the other products of operators can also be obtained. For spontaneous emission, the photon bath is assumed to be in equilibrium. The expectation value $\langle X_t X_{t'}^\dagger \rangle_0 \equiv C(t-t')$ is a function of the time interval only. We can now define the Laplace transformation for real $z$,

$$C_\varepsilon(z) \equiv \int_0^\infty dt e^{-zt} e^{i\varepsilon t} C(t),$$

$$n_U(z) \equiv \int_0^\infty dt e^{-zt} \langle \hat{n}_U \rangle_t, \quad \text{etc.,} \quad z>0 \tag{6}$$

and transform the whole equations of motion into $z$ space

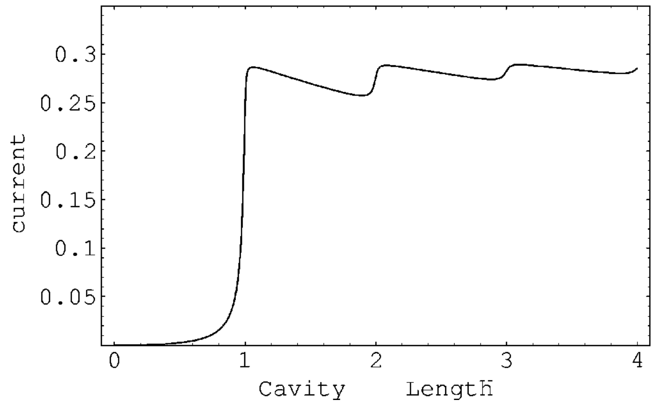


FIG. 2. Stationary tunnel current, Eq. (8), as a function of cavity length $L_c$. The vertical and horizontal units are 100 pA and $\lambda_0$, respectively.

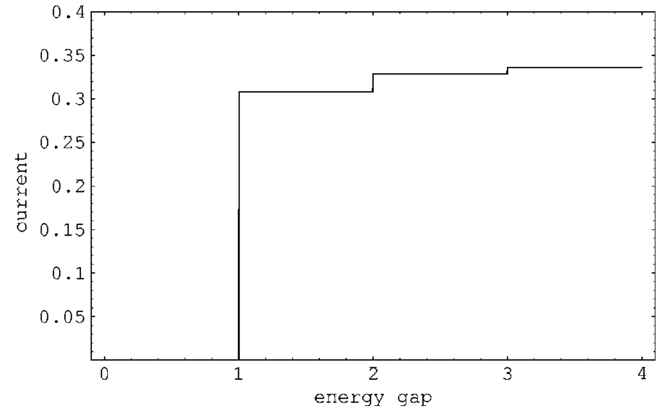


FIG. 3. Stationary current as a function of exciton energy gap $\varepsilon$. The cavity length is fixed to $\lambda_0/2$. The current is in units of 100 pA, while the energy gap is terms of $2hc/\lambda_0$.

$$n_U(z) = -i\frac{g}{z}[p(z)-p^*(z)] + 2\frac{\Gamma_U}{z}[1/z - n_U(z) - n_D(z)],$$

$$n_D(z) = \frac{g}{z}[p(z)-p^*(z)] - 2\frac{\Gamma_D}{z}n_D(z), \tag{7}$$

$$p(z) = -ig\{n_U(z)C_\varepsilon(z) - n_D(z)C^*_{-\varepsilon}(z)\} - \Gamma_D p(z)C_\varepsilon(z),$$

$$p^*(z) = ig\{n_U(z)C^*_\varepsilon(z) - n_D(z)C_{-\varepsilon}(z)\} - \Gamma_D p^*(z)C^*_\varepsilon(z).$$

These equations can then be solved algebraically. The tunnel current $\hat{I}$ can be defined as the change of the occupation of $\hat{n}_U$ and is given by $\hat{I} \equiv ig(\hat{p}-\hat{p}^\dagger)$, where we have set the electron charge $e=1$ for convenience. The time dependence of the expectation value $\langle \hat{I} \rangle_t$ can be obtained by solving Eq. (7) and performing the inverse Laplace transformation. For time $t \to \infty$, the result is

$$\langle \hat{I} \rangle_{t\to\infty} = \frac{2g^2\Gamma_U\Gamma_D B}{g^2\Gamma_D B + [g^2 B + \Gamma_D + 2\gamma\Gamma_D^2 + (\gamma^2+\Omega^2)\Gamma_D^3]},$$

$$B = \gamma + (\gamma^2 + \Omega^2)\Gamma_D, \tag{8}$$

where $g^2\Omega$ and $g^2\gamma$ are the exciton frequency shift and decay rate, respectively. The derivation of the current equation is closely analogous to the spontaneous emission of phonons in double dots,[23] in which the correlation functions $\langle X_t X^\dagger_{t'} \rangle_0$ are given by the electron-phonon interaction.

Since the stationary current through the quantum dot depends strongly on the decay rate $\gamma$, the results of a quantum dot inside a planar microcavity is numerically displayed in Fig. 2. In plotting the figure, the current is in terms of 100 pA, and the cavity length is in units of $\lambda_0/2$, where $\lambda_0$ is the wavelength of the emitted photon. Furthermore, the tunneling rates $\Gamma_U$ and $\Gamma_D$ are assumed to be equal to $0.2\gamma_0$ and $\gamma_0$, respectively. Here, a value of 1/1.3 ns for the free-space quantum dot decay rate $\gamma_0$ is used in our calculations.[19] Also, the planar microcavity has a Lorentzian broadening at each resonant modes (with broadening widths equal to 1% of each resonant mode).[17] As the cavity length is less than half of the wavelength of the emitted photon, the stationary current is inhibited. This is because the energy of the photon generated by the quantum dot is less than the cutoff frequency of the planar microcavity. Moreover, the current is increased whenever the cavity length is equal to the multiple half wavelength of the emitted photon. As the cavity length exceeds some multiple wavelength, it opens up another decay channel abruptly for the quantum dot exciton, and it turns out that the current is increased. With the increasing of cavity length, the stationary current becomes less affected by the cavity and gradually approaches the free space limit.

To understand the inhibited current thoroughly, we now fix the cavity length equal to $\lambda_0/2$ and vary the exciton energy gap, while the planar microcavity is now assumed to be perfect. The vertical and horizontal units in Fig. 3 are 100 pA and $2hc/\lambda_0$, respectively. Here, $\lambda_0$ is the wavelength of the photon emitted by the quantum dot exciton in free space. Once again, we observe the suppressed current as the exciton energy gap is tuned below the cutoff frequency. The plateau features in Fig. 3 also come from the abruptly opened decay channels for the quantum dot exciton. From an experimental point of view, it is not possible to tune either the cavity length or the energy gap for such a wide range. A possible way is to vary the exciton gap around the first discontinuous point $2hc/\lambda_0$. Since the discontinuities should smear out for the real microcavity, it is likely to have a peak if one measures the differential conductance $d\langle \hat{I} \rangle/d\varepsilon$ as a function of energy gap $\varepsilon$.

The coherence of the quantum states is a fundamental issue in quantum physics. The decoherence caused by phonons or imperfections may destroy the unitary quantum evolution. The atomic exciton ground state of an isolated quantum dot has recently been shown to be radiatively damped. Coupling with acoustical phonons or imperfections plays no role during the exciton lifetime.[25] Therefore, our proposal can also be used to measure the super-radiance of quantum dots in an electrical way. Consider now the system containing two quantum dots with a distance $d$. One of the obstacles in measuring the super-radiance between the quantum dots comes from the random size of the dots which result in a random distribution of energy gap. This can be

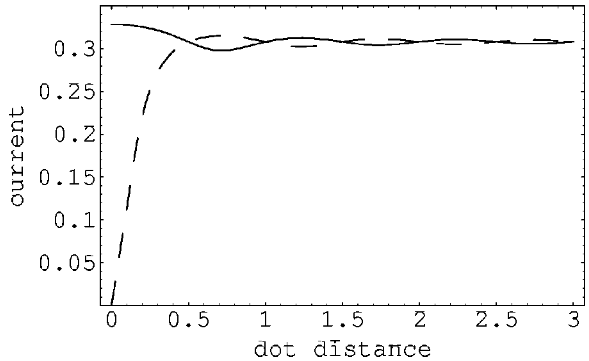


FIG. 4. Stationary current (in units of 100 pA) through the superradiant (solid line) and subradiant (dashed line) channel as a function of dot distance $d$ (in units of $\lambda_0$).

overcome by growing two gates above the quantum dots. The energy gap and the orientation of the dipole moments can be controlled well. Analogous to the two-ion system,[24] the electron and hole can tunnel into the super-radiant or subradiant state. The corresponding decay rate for the two channels is given by

$$\gamma_{\pm}=\gamma_0\left(1\pm\frac{\sin(2\pi d/\lambda_0)}{2\pi d/\lambda_0}\right), \tag{9}$$

where the two signs $\pm$ correspond to the two different relative orientations of the dipole moments of the two dots. Figure 4 shows the stationary currents of the super-radiant (solid line) and subradiant (dashed line) channels. The interference effect between the dots is displayed explicitly. In principle, one can incorporate more quantum dots in the system, and many super-radiant effects can be examined by the electrical current.

In conclusion, we have proposed a method of detecting the Purcell effect in a semiconductor quantum dot system. By incorporating the InAs quantum dot between a $p$-$i$-$n$ junction surrounded by a planar microcavity, the Purcell effect on stationary tunnel current can be examined either by changing the cavity length or by varying the exciton energy gap. Second, it is also possible to observe super-radiant effects between two dots by using the present model. The interference features are pointed out and may be observable in a suitably designed experiment.

We would like to thank to Professor D. A. Rudman and Professor M. Keller of NIST for helpful discussions. One of authors (Y. N. Chen) also appreciate valuable discussions with P. C. Chen of UCSD. This work is supported partially by the National Science Council, Taiwan under Grant No. NSC 91-2112-M-009-012.

## APPENDIX A: DERIVATION OF THE EQUATIONS OF MOTION

In this appendix, we will derive a master equation from the exact time evolution of the system. We will assume that couplings to the left and right electron reservoirs are weak and a standard Born-Markov approximation with respect to these couplings is reasonable. The assumption of weak reservoir coupling means that we neglect the effects aroused from higher order tunneling such as cotunneling processes throughout. In particular, we are outside the regime of strong coupling to the leads where signatures of the Kondo effect start to play a role.

Now, we define an interaction picture for arbitrary operator $\hat{O}$ and by the $X$ operator by

$$\tilde{O}(t)\equiv e^{iH_0t}Oe^{-iH_0t}, \quad X_t\equiv e^{iH_0t}Xe^{-iH_0t}. \tag{A1}$$

Furthermore, for the total density matrix $\Xi(t)$ which obeys the Liouville equation

$$\Xi(t)=e^{-iHt}\Xi_{t=0}e^{iHt}, \tag{A2}$$

we define

$$\tilde{\Xi}(t)\equiv e^{iH_0t}\Xi(t)e^{-iH_0t}. \tag{A3}$$

The expectation value of any operator $\hat{O}$ is given by

$$\langle\hat{O}\rangle_t\equiv \mathrm{Tr}[\Xi(t)O]=\mathrm{Tr}[\tilde{\Xi}(t)\tilde{O}(t)]. \tag{A4}$$

We therefore have

$$\begin{gathered}\tilde{n}_U(t)=\hat{n}_U, \quad \tilde{n}_D(t)=\hat{n}_D,\\ \tilde{p}(t)=\hat{p}e^{i\varepsilon t}X_t, \quad \tilde{p}^{\dagger}(t)=\hat{p}^{\dagger}e^{-i\varepsilon t}X_t^{\dagger},\\ \varepsilon\equiv\varepsilon_U-\varepsilon_D.\end{gathered} \tag{A5}$$

The equation of motion for $\tilde{\Xi}(t)$ becomes

$$i\frac{d}{dt}\tilde{\Xi}(t)=[\tilde{H}_T(t)+\tilde{H}_V(t),\tilde{\Xi}(t)]. \tag{A6}$$

This can be written as

$$\begin{aligned}\frac{d}{dt}\tilde{\Xi}(t)=-i[\tilde{H}_T(t),\tilde{\Xi}(t)]-i[\tilde{H}_V(t),\tilde{\Xi}(t)]=\\ -i[\tilde{H}_T(t),\tilde{\Xi}(t)]-i[\tilde{H}_V(t),\Xi_0]\\ -\int_0^t dt'\{\tilde{H}_V(t),[\tilde{H}_T(t')+\tilde{H}_V(t'),\tilde{\Xi}(t')]\}.\end{aligned} \tag{A7}$$

Now, we define the effective density operator of the dot plus photons

$$\tilde{\rho}(t)=\mathrm{Tr}_{\mathrm{res}}\tilde{\Xi}(t) \tag{A8}$$

as the trace of $\tilde{\Xi}(t)$ taking over electron reservoirs. The trace $\mathrm{Tr}_{\mathrm{res}}$ taking over the terms linear in $H_V$ vanishes, therefore,

$$\begin{aligned}\frac{d}{dt}\tilde{\rho}(t)=-i[\tilde{H}_T(t),\tilde{\rho}(t)]\\ -\mathrm{Tr}_{\mathrm{res}}\int_0^t dt'\{\tilde{H}_V(t),[\tilde{H}_V(t'),\tilde{\Xi}(t')]\}.\end{aligned} \tag{A9}$$

As can be seen from the above equation, the last term is already second order in $H_V$, we can approximate

$$\tilde{\Xi}(t')\approx R_0\tilde{\rho}(t'), \tag{A10}$$

where $R_0$ is the equilibrium density matrix for the two electron reservoirs. Working out the commutators and using the time evolution of the electron reservoir operators

$$\tilde{c}_{\mathbf{q}}(t)=e^{-i\varepsilon^U_{\mathbf{q}}t}c_q, \quad \tilde{d}_{\mathbf{q}}(t)=e^{-i\varepsilon^D_{\mathbf{q}}t}d_q, \tag{A11}$$

the master equation becomes

$$\begin{aligned}\tilde{\rho}(t)=&\rho_0-i\int_0^t dt'[\tilde{H}_T(t'),\tilde{\rho}(t')]\\&-\Gamma_U\int_0^t dt'\{\widetilde{s_U}(t')\widetilde{s_U}^\dagger(t')\tilde{\rho}(t')\\&-2\widetilde{s_U}^\dagger(t')\tilde{\rho}(t')\widetilde{s_U}(t')\}\\&-\Gamma_U\int_0^t dt'\{\tilde{\rho}(t')\widetilde{s_U}(t')\widetilde{s_U}^\dagger(t')\}\\&-\Gamma_D\int_0^t dt'\{\widetilde{s_D}^\dagger(t')\widetilde{s_D}(t')\tilde{\rho}(t')\}-\Gamma_D\int_0^t dt'\\&\times\{-2\widetilde{s_D}(t')\tilde{\rho}(t')\widetilde{s_D}^\dagger(t')+\tilde{\rho}(t')\widetilde{s_D}^\dagger(t')\widetilde{s_D}(t')\},\end{aligned} \tag{A12}$$

where $\Gamma_U=2\pi\Sigma_{\mathbf{q}}V^2_{\mathbf{q}}\delta(\varepsilon_U-\varepsilon^U_{\mathbf{q}})$, $\Gamma_D=2\pi\Sigma\mathbf{q}W^2_{\mathbf{q}}\delta(\varepsilon_D-\varepsilon^D_{\mathbf{q}})$.

Multiplying Eq. (A12) by $\hat{n}_U$, $\hat{n}_D$, $\hat{p}$, and $\hat{p}^\dagger$, respectively and performing the trace with the three dot states in Eq. (1), one obtains

$$\begin{aligned}\langle\hat{n}_U\rangle_t-\langle\hat{n}_U\rangle_0=&-ig\int_0^t dt'\{\langle\hat{p}\rangle_{t'}-\langle\hat{p}^\dagger\rangle_{t'}\}\\&+2\Gamma_U\int_0^t dt'(1-\langle\hat{n}_U\rangle_{t'}-\langle\hat{n}_D\rangle_{t'}),\\\langle\hat{n}_D\rangle_t-\langle\hat{n}_D\rangle_0=&-ig\int_0^t dt'\{\langle\hat{p}\rangle_{t'}-\langle\hat{p}^\dagger\rangle_{t'}\}\\&-2\Gamma_D\int_0^t dt'\langle\hat{n}_D\rangle_{t'},\\\langle\hat{p}\rangle_t-\langle\hat{p}\rangle^0_t=&-\Gamma_D\int_0^t dt'e^{i\varepsilon(t-t')}\langle X_tX^\dagger_{t'}\tilde{p}(t')\rangle_{t'}\\&-ig\int_0^t dt'e^{i\varepsilon(t-t')}\{\langle\hat{n}_UX_tX^\dagger_{t'}\rangle_{t'}\\&-\langle\hat{n}_DX^\dagger_{t'}X_t\rangle_{t'}\},\\\langle\hat{p}^\dagger\rangle_t-\langle\hat{p}\rangle^0_t=&-\Gamma_D\int_0^t dt'e^{-i\varepsilon(t-t')}\langle\tilde{p}^\dagger(t')X_{t'}X^\dagger_t\rangle_{t'}\\&+ig\int_0^t dt'e^{-i\varepsilon(t-t')}\{\langle\hat{n}_UX_{t'}X^\dagger_t\rangle_{t'}\\&-\langle\hat{n}_DX^\dagger_tX_{t'}\rangle_{t'}\}.\end{aligned} \tag{A13}$$

---

*Electronic address: ynchen.ep87g@nctu.edu.tw

†Electronic address: dschuu@cc.nctu.edu.tw

[1] E. M. Purcell, Phys. Rev. **69**, 681 (1946).
[2] P. Goy, J. M. Raimond, M. Gross, and S. Haroche, Phys. Rev. Lett. **50**, 1903 (1983).
[3] G. Gabrielse and H. Dehmelt, Phys. Rev. Lett. **55**, 67 (1985).
[4] R. G. Hulet, E. S. Hilfer, and D. Kleppner, Phys. Rev. Lett. **55**, 2137 (1985).
[5] D. J. Heinzen, J. J. Childs, J. E. Thomas, and M. S. Feld, Phys. Rev. Lett. **58**, 1320 (1987).
[6] J. J. Hopfield, Phys. Rev. **112**, 1555 (1958).
[7] V. Agranovich and O. Dubovsly, JETP Lett. **3**, 223 (1966).
[8] K. C. Liu and Y. C. Lee, Physica A **102A**, 131 (1980).
[9] E. Hanamura, Phys. Rev. B **38**, 1228 (1988).
[10] J. Knoester, Phys. Rev. Lett. **68**, 654 (1992).
[11] D. S. Citrin, Phys. Rev. B **47**, 3832 (1993).
[12] G. Björk, Stanely Pau, Joseph M. Jacobson, H. Cao, and Y. Yamamoto, Phys. Rev. B **52**, 17 310 (1995).
[13] Y. N. Chen and D. S. Chuu, Phys. Rev. B **61**, 10 815 (2000); Europhys. Lett. **54**, 366 (2001).
[14] Y. Yamamoto, S. Machida, K. Igeta, and Y. Horikoshi, *Coherence and Quantum Optics*, edited by E. H. Eberly *et al.* (Plenum Press, New York, 1989), Vol. VI, p. 1249.
[15] C. Constaintin, E. Martinet, A. Rudra, and E. Kapon, Phys. Rev. B **59**, R7809 (1999).
[16] Y. C. Lee, D. S. Chuu, and W. N. Mei, Phys. Rev. Lett. **69**, 1081 (1992).
[17] Y. N. Chen, D. S. Chuu, T. Brandes, and B. Kramer, Phys. Rev. B **64**, 125307 (2001).
[18] J. M. Gerard *et al.*, Phys. Rev. Lett. **81**, 1110 (1998).
[19] G. S. Solomon, M. Pelton, and Y. Yamamoto, Phys. Rev. Lett. **86**, 3903 (2001).
[20] M. Bayer, Phys. Rev. Lett. **86**, 3168 (2001).
[21] O. Benson, C. Santori, M. Pelton, and Y. Yamamoto, Phys. Rev. Lett. **84**, 2513 (2001).
[22] Z. Yuan, B. E. Kardynal, R. M. Stevenson, A. J. Shields, C. J. Lobo, K. Cooper, N. S. Beattie, D. A. Ritchie, and M. Pepper, Science **295**, 102 (2002).
[23] T. Brandes and B. Kramer, Phys. Rev. Lett. **83**, 3021 (1999).
[24] R. G. DeVoe and R. G. Brewer, Phys. Rev. Lett. **76**, 2049 (1996).
[25] T. Flissikowski, A. Hundt, M. Lowisch, M. Rabe, and F. Henneberger, Phys. Rev. Lett. **86**, 3172 (2001).